

Article

The Contribution of Groundwater to the Salinization of Reservoir-Based Irrigation Systems

Michiele Gebrehiwet ¹, Nata T. Tafesse ^{2,*} , Solomon Habtu ¹, Berhanu F. Alemaw ² ,
Kebabonye Laletsang ² and Reneilwe Lasarwe ²

¹ Department of Land Resource Management and Environmental Protection, College of Dryland Agriculture and Natural Resources, P.O. Box 231, Mekelle University, Mekelle, Ethiopia; gemikmah@gmail.com (M.G.); solomon.habtu@mu.edu.et (S.H.)

² Geology Department, University of Botswana, Private Bag UB 00704, Gaborone, Botswana; Alemaw@ub.ac.bw (B.F.A.); laletsak@ub.ac.bw (K.L.); lasarwe@ub.ac.bw (R.L.)

* Correspondence: tafessen@ub.ac.bw

Abstract: This study evaluates the cause of salinization in an irrigation scheme of 100 ha supplied from a reservoir. The scheme is located in Gumselasa catchment (28 km²), Tigray region, northern Ethiopia. The catchment is underlain by limestone–shale–marl intercalations with dolerite intrusion and some recent sediments. Water balance computation, hydrochemical analyses and irrigation water quality analyses methods were used in this investigation. Surface waters (river and reservoir) and groundwater samples were collected and analyzed. The water table in the irrigated land is ranging 0.2–2 m below the ground level. The majority of groundwater in the effective watershed area and the river and dam waters are fresh and alkaline whereas in the command area the groundwater is dominantly brackish and alkaline. The main hydrochemical facies in the groundwater in the effective watershed area are Ca-Na-SO₄-HCO₃, Ca-Na-HCO₃-SO₄, and Ca-Na-Mg-SO₄-HCO₃. The river and dam waters are Mg-Na-HCO₃-SO₄ and HCO₃-SO₄-Cl types, respectively. In the command area the main hydrochemical facies in the groundwater are Ca-Na-HCO₃-SO₄ and Ca-Na-Mg-SO₄-HCO₃. Irrigation water quality analyses revealed that salinity and toxicity hazards increase from the effective watershed to the irrigated land following the direction of the water flow. The results also showed that the analyzed waters for irrigation purpose had no sodicity hazard. The major composition controlling mechanisms in the groundwater chemistry was identified as the dissolution of carbonate minerals, silicate weathering, and cation exchange. One of the impacts of the construction of the dam in the hydrologic environment of the catchment is on its groundwater potential. The dam is indirectly recharging the aquifers and enhances the groundwater potential of the area. This increment of availability of groundwater enhanced dissolution of carbonate minerals (calcite, dolomite, and gypsum), silicate weathering and cation exchange processes, which are the main causes of salinity in the irrigated land. The rising of the brackish groundwater combined with insufficient leaching contributed to secondary salinization development in the irrigated land. Installation of surface and subsurface drainage systems and planting salt tolerant (salt loving) plants are recommended to minimize the risk of salinization and salt accumulation in the soils of the irrigated land.

Keywords: groundwater; irrigation; salinity; sodicity; toxicity



Citation: Gebrehiwet, M.; Tafesse, N.T.; Habtu, S.; Alemaw, B.F.; Laletsang, K.; Lasarwe, R. The Contribution of Groundwater to the Salinization of Reservoir-Based Irrigation Systems. *Agronomy* **2021**, *11*, 512. <https://doi.org/10.3390/agronomy11030512>

Academic Editors:
Willibald Loiskandl and
Peter Langridge

Received: 29 December 2020
Accepted: 26 February 2021
Published: 10 March 2021

Publisher's Note: MDPI stays neutral with regard to jurisdictional claims in published maps and institutional affiliations.



Copyright: © 2021 by the authors. Licensee MDPI, Basel, Switzerland. This article is an open access article distributed under the terms and conditions of the Creative Commons Attribution (CC BY) license (<https://creativecommons.org/licenses/by/4.0/>).

1. Introduction

1.1. General

Salinization refers to a rise of excess soluble salts concentration in the soil. These salts occur in the soil as ions: Cl⁻, SO₄²⁻, HCO₃⁻, CO₃²⁻, NO₃⁻, Na⁺, Ca²⁺, Mg²⁺, and K⁺. Salinization occurs in nearly all climatic regions in non-irrigated areas, irrigated areas, and coastal areas. It can be caused by geogenic processes and anthropogenic impacts [1]. In the non-irrigated area, which is common in dryland regions and is known as dryland salinity,

the cause is the rising of brackish/saline groundwater to the surface or depth of root zone from unconfined, perched, or leaky aquifers. Unavailability of sufficient rainfall to flush the soils and the existence of high evapotranspiration rate has led the salts in brackish/saline groundwater to accumulate in the soils. In irrigated areas consist of waterlogged soils usage of brackish/saline water from a reservoir and/or brackish/saline groundwater from wells for irrigation is the cause of salinization. The rises of brackish/saline groundwater to the depth of the root zone from an unconfined aquifer, perched aquifer, or leaky aquifer may also cause salinization in irrigated areas covered by poorly drained soils. In coastal areas it can be caused due to flooding of the land by seawater and salt water intrusions. In all these areas a practice of excessive fertilization with very soluble forms of fertilizer and excessive usage of pesticides can cause salinization. Evangelou [2], in his publication, "Effects of Fertilizer Salts on Crop Production" had shown that excessive usage of fertilizers result salt toxicities that severely injure the growth and development of plants. The author also showed that soluble fertilizers differ in the degree to which they contribute to the process of salinization.

Salinization is a worldwide problem. According to Szabolcs [3] there is no continent in this world that does not have salt-affected soils and at least seventy countries have major salt-related problems. In a study carried out by Pooja and Rajesh [4] on development of simple and low cost biological methods for salinity stress management, it was shown that worldwide out of the entire irrigated and cultivated agricultural lands 33% and 20%, respectively, are estimated to be affected by high salinity.

Among the worldwide distributed salt-affected areas, the largest area is found in arid and semi-arid regions [5,6], where poor quality groundwater is used for irrigation and evapotranspiration rate is very high. Mateo-Sagasta and Burke [7], in their report on agriculture and water quality interactions at a global scale, had shown that 25% of the total irrigated land is affected by soil degradation due to the impact of high to moderate salinization in the Mediterranean area. In Europe about 3.8 million hectares are affected by soil salinization [8]. Zaman et al. [1], in their publication on guideline on protocols for salinity and sodicity assessment, and the role of isotopic nuclear and related techniques to develop mitigation and adaptation measures to use saline and sodic soils sustainably, reported that 20% of the cultivable land is affected by sodicity or salinity in India, 10 million hectares are affected by soil salinization in Pakistan and in Africa the total area of human-induced salt-affected soils is 14.8 million hectares. Pooja and Rajesh [4] state that, globally, the extents of salt-affected areas are increasing at a rate of 10% annually for numerous reasons.

In Ethiopia, salinization affects more than 11 million of hectares of land [9–12] that are dominantly located in the Ethiopian Rift Valley and other semi-arid and arid parts of the country. The study area for the Gumselasa irrigation scheme is located in Gumselasa catchment, in the highlands of Tigray region, which is a drought prone and degraded region of Ethiopia [13]. The dam was constructed twenty-five years ago for an irrigation purpose. The history of the Gumselasa catchment shows that the current irrigated area and reservoir site were cultivated land where local communities practiced rainfed agriculture [14] without any record of the salinization problem. The current irrigated area, located in the downstream side of the dam, stretched from the area around the dam to the outlet of the catchment. The catchment is a sub catchment of May Taweru river, a tributary of the Tekeze river, which in turn is a major tributary of the Atbarah river (Black Nile) in Sudan.

Since the commencement of the dam operation, the farmers are benefitting from the irrigation scheme. In a study carried out by Teshome [15] on the state irrigation interventions interface with irrigators' life-worlds in a drought-prone region of Northern Ethiopia by taking the Gumselasa irrigation system as a case study area, it was shown that following the operation of the dam, in the years from 2000 to 2005, the mean production of maize has increased from 24 to 167.5 quintals per hectare. However, from year to year there is a reduction of the land size covered by the irrigation due to salinization, which led

to a reduction in the annual production of the farmers. Currently more than 10 ha of land of the command area is abandoned because of salinization.

The irrigation scheme has been studied by many scholars and researchers [13–29]. Most these studies have focused on irrigation water management and on socioeconomic aspects and few of them considered salinity developments and relate its source with poor agricultural water management practices. A detail study on the causes of salinity by taking into account the geology and the hydrochemical nature of the groundwater of the catchment is lacking. Identifying the exact source of salinity is essential to determine and design appropriate methods to control soil salinity and also restore salt-affected soils. This research was done with the objective to identify the cause of salinity in the Gumselasa irrigation scheme by considering the underlain geological units and the hydrochemical nature of the groundwater of the area.

1.2. The Study Area

1.2.1. Location

Gumselasa irrigation scheme is located in Gumselasa catchment (28.1 km²) in the southern administrative zone of the Tigray region, North Ethiopia. Geographically, it is found bounded between 556,000–564,000 m E and 1,458,000–1,467,000 m N (Figure 1).

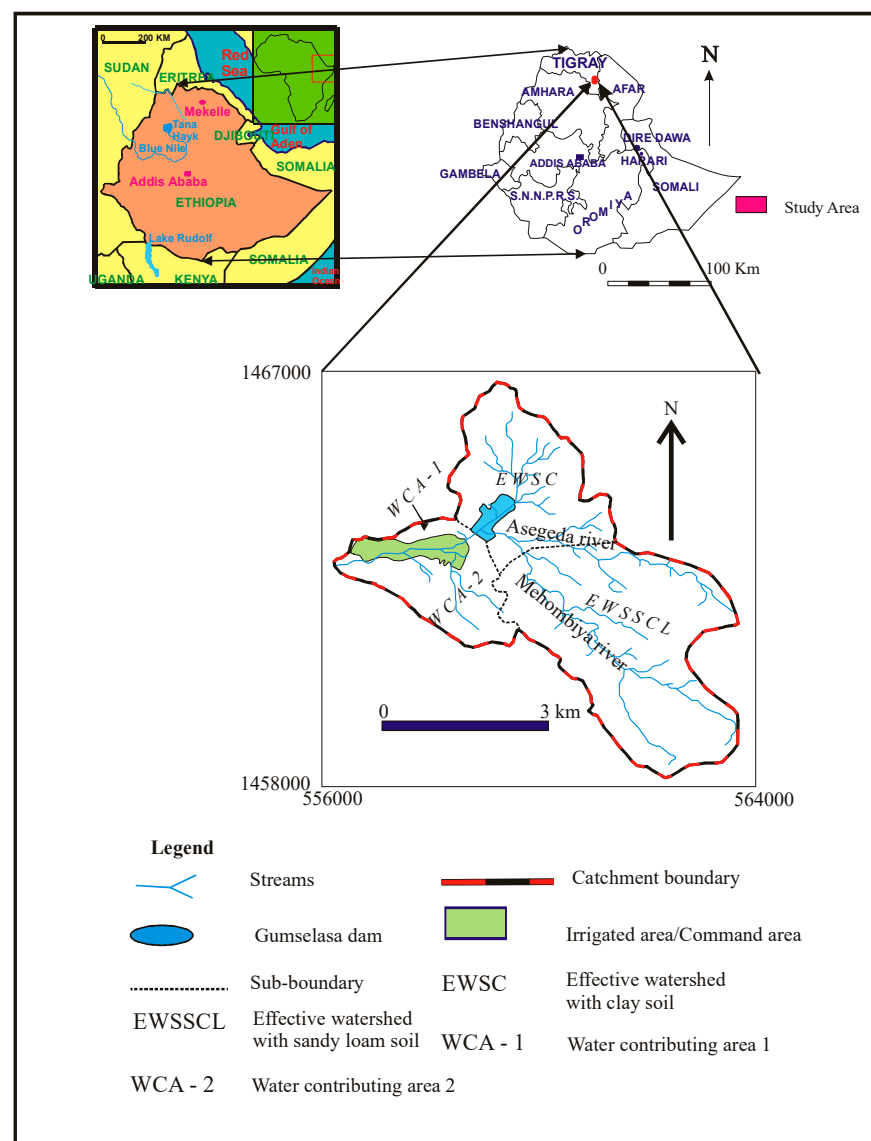


Figure 1. Location map of the study area (source: modified after Nata [30]).

The catchment is mainly gentle to flat sloping area and is drained by Mehombiya and Asegeda rivers, which are perennial and main rivers in the catchment. Both of them rise from surrounding mountains: Mehombiya from the southeast and flows to the west whereas Asegeda from east and flows to southwest (Figure 1). Besides to these rivers, the catchment is also drained by other minor seasonal streams.

Gumselasa dam, which is the sole source of irrigation water for the irrigation scheme, was constructed across these rivers in 1995 [14] and commenced its operation after two years [18] with a height of 13.5 m, 400 m dam axis length, reservoir capacity of 1.92 million cubic meters, and a command area for irrigation of 120 ha [14,26]. Currently the available water in the dam is 0.194 million cubic meters and the area covered by irrigation is 100 ha.

1.2.2. Geology

Geologically the study area is mainly constituted by a limestone–shale–marl intercalation with dolerite intrusion and Quaternary sediments [29] (Figure 2). The underlying limestone–shale–marl intercalation unit is part of the Mesozoic sedimentary succession of Northern Ethiopia, which consists of a gray-green and black shale, marl, and claystone interlaminated with finely crystalline black limestone containing disseminated pyrite with some gastropods and brachiopods [31–35]. According to Enkurie [34] it also contains some thin beds of gypsum and dolomite and a few beds of yellow coquina.

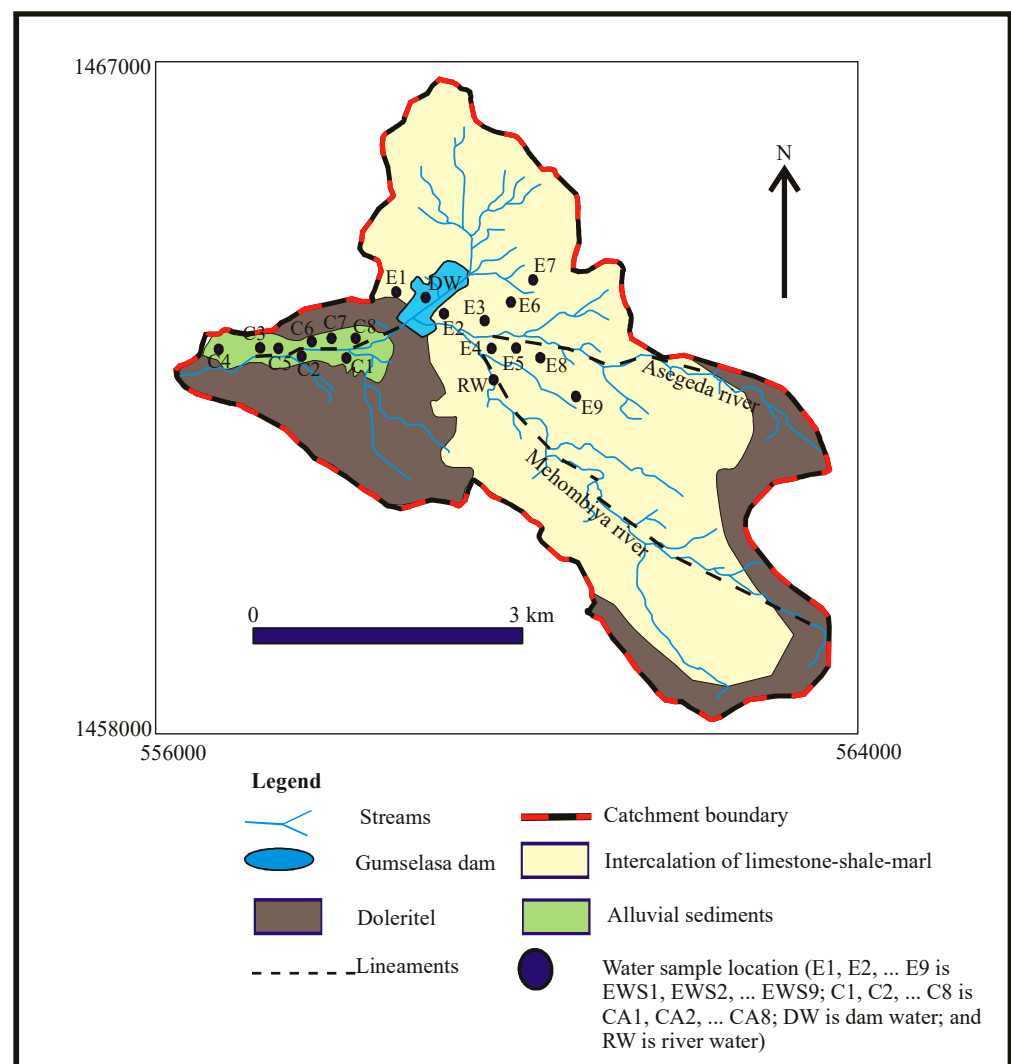


Figure 2. Geological map of the catchment.

Limestone–Shale–Marl Intercalation

This unit is outcropped mainly in the northeastern, southern, northern, western, and central parts of the catchment. It is found forming moderately steep to gentle and flatland areas and poorly exposed.

It is consisting of light yellowish and greenish gray shale intercalated with thinly bedded, light gray to yellowish marl, and thick, finely crystalline limestone with occasional patches of gypsum. The unit is generally dominated by shale and marls in various proportions. The exposed thickness of each shale bed is ranging from 0.2 to 5 m, and it is poorly weathered. The thickness of the intercalated limestone is ranging from 0.3 to 1 m. The limestone is fossiliferous, fractured, and weathered. Secondary precipitated calcium carbonate due to dissolution and recrystallization of calcite is common in this unit (Figure 3).



Figure 3. Exposed limestone–shale–marl intercalation in the command area.

Mineralogically, the intercalated limestone is composed mainly of calcite (80–56%), quartz (6–2%), opaque (Fe–oxide) (3%), feldspar (2–1%), gypsum (2% to nil), and sphene (1% to nil). Its fossil content ranges from trace to 32% [36].

Dolerites Dykes

Numerous dolerite dykes that are intruding the limestone–shale–marl intercalation units occur in the catchment. These intrusions are black andesine dolerite with ophitic texture and outcropped mainly in the eastern, western, southwestern, southern, and southeastern parts of the catchment.

They are forming a dome like spheroid shape in most case and in some case they are exposed as dykes dominantly having a trend of N-S in the eastern and central parts of the catchment. They also occur as irregular bodies within the sedimentary successions in different parts of the catchment. The weathered part of this dolerite dyke exposes a circular boulder resulting from spheroidal (exfoliation) weathering. In the southeastern and eastern sides of the catchment and also in the area where the crest of the dam is located, the dolerite surface is covered by precipitated calcium carbonate (Figure 4). This is the result of dissolution and recrystallization calcite while dolerite is intruding through the limestone–marl–shale intercalation.



Figure 4. Calcium carbonate precipitated on the dolerite at the eastern flank of the effective watershed.

Mineralogically, the rocks are composed of plagioclase (46–40%), pyroxene (37–32%), opaque (Fe-oxide) (10–8%), biotite (8–2%), apatite (10% to nil), and olivine (7% to nil) [36].

Quaternary Deposits

In the catchment, extensive Quaternary sediment areas are not available. Mappable Quaternary sediments are found in variable thickness and areal extent mainly in the command area. Elsewhere bedrocks are variably covered by earthy soils. In the command area, the sediments are mainly black to brownish clay that has a thickness greater than 3 m. The sediments do not have the same thickness throughout the command area.

Less extensive unconsolidated sediments occur in the northeast, north, and northwest parts of the catchment covering the relatively flat areas. These sediments are formed by the processes of weathering from the underlying bedrocks. The sediments are mainly black cotton soil, which being rich in clay and their thickness range from 2 to 5 m.

Along the margins of the Asegeda and Mehombiya rivers and their tributaries alluvium are found as thin strips. The relative abundances and stratigraphic relations of these sediments, however, are generally not uniform throughout the catchment. Toward the mountains front, where the gradient of the rivers is high and steep topographic slopes exist, the alluvium, in general, are dominated by coarse grained subrounded to subangular particles mixed with coarse grained sand. In the eastern, southeastern, and southern parts of the catchment, where the gradient of the rivers decreases down slope, the dominant alluvium are fine to medium grained sand particles mixed with variable content of fine grained sediments. The thickness of this alluvial deposit ranges from 0.5 to 6 m.

1.2.3. Water Uses

The study area is endowed with both surface water and groundwater. River water and dam water represents the surface water resource of the area.

In the study area groundwater is the main source of water supply for domestic use. More than 10 closed hand dug wells (Figure 5b) exist in different parts of the upstream side of the dam for this purpose. Besides, two deep wells that have a depth of 120 m and 45 m exist in the downstream side of the dam immediately behind the main structure of the dam [29]. Of these two deep wells, due to poor quality of the groundwater, the deep well that has a depth of 120 m is sealed and abandoned. The latter currently serve as a source of water for domestic water supplies for the nearby town and villages. There is no hand dug well in the downstream side of the dam.



Figure 5. Some of the existing opened hand-dug well (a) and closed hand dug well (b) in the effective watershed area.

Groundwater is also used as a source of irrigation water in the upstream side of the dam. However, agricultural activities in this part of the catchment are dominantly rainfed. Only few numbers of farmers are practicing an irrigation activities using groundwater as a source of irrigation water from open hand dug wells (Figure 5a) since 2005 with no record of major salinization problem and history of abandoned land due to this problem [29].

The majority of open hand dug wells have trapezoidal shape with an upper diameter ranging from 5 to 9 m and final internal diameter ranging from 2 to 5 m. The depth of the hand dug wells varies between 5 to 15 m. The depth of static water levels ranges from 3 to 11 m. In closed hand dug wells water abstraction is done with hand pumps (Figure 5a) while treadle and motor pumps (Figure 6) are used in the open hand dug wells.



Figure 6. Groundwater abstraction using the treadle pump.

The shallow, mostly perched, aquifers in the thin alluvial covers and the upper weathered and fractured zones of the underlying rocks (limestone–shale–marl intercalation) are exploited through these hand dug wells. Those hand dug wells that are tapping only the alluvial aquifer are characterized by a groundwater quality having a TDS < 1000 mg/L whereas those that are tapping by including the next lower or underlying water bearing stratum are characterized by brackish quality nature. The majority of the hand dug wells are often dry during the peak time of the dry season of the year.

Irrigated agriculture is the main agricultural activity in the downstream side of the dam with the dam water as the only source of water for the irrigation. Groundwater is not used as a source of irrigation water in this part of the catchment.

2. Methods

2.1. Data Collection

The whole catchment boundary and specific boundaries (effective watershed area, reservoir area, command area, and adjacent water contributing areas to the command area; Figure 1) delineations were done using Garmin GPS and topographic map with a scale of 1:50,000 as a base map. Different maps were prepared using the readings and the topographic map as a base map.

Geological investigation was done in the field paying particular attention to the water bearing nature of the rocks and sediments in the side and surrounding area of the catchment.

Computation of the water balance of the catchment was done by the same authors of this paper [27] and was used here as input data for the analyses the causes of salinization.

Eight test pits were excavated for collection of groundwater samples and to measure the depth to groundwater in different parts of the command area (Figure 7). The pits size was 1 m by 1 m having a depth ranging from 1.4 to 3.5 m.



Figure 7. Some of the test pits in the command area.

For hydrochemical and irrigation water analyses, representative samples were collected from all the water resources of the study area. Accordingly, nineteen water samples were collected from the different parts of the catchment: nine groundwater samples from existing opened hand dug wells (Figure 5a) and one sample from river in the effective watershed area, one sample from reservoir and eight groundwater samples from test pits in the command area (Figure 7). Before sampling the groundwater, the hand dug wells and

pits identified for this purpose were purged for about 5 min to ensure that the standing water did not contaminate the sample and that the water that was sampled was from the aquifer. All the groundwater samples are shallow groundwater and were collected at low water levels manually. The sampling was done during the dry season of the year before the peak time of the season. For all the samples, TDS, EC, pH, and temperature of the water were measured in situ using a digital multiparameter analyzer.

2.2. Data Analysis

Surface water and groundwater samples were analyzed at the Department of Earth Science geochemistry laboratory in Mekelle University, Ethiopia. The samples were analyzed for calcium (Ca^{2+}), magnesium (Mg^{2+}), potassium (K^+), sodium (Na^+), bicarbonate (HCO_3^-), chloride (Cl^-), sulfate (SO_4^{2-}), and nitrate (NO_3^-). A flame photometer and atomic absorption spectrophotometer (AAS) were used for analyses of Na^+ , K^+ , Ca^{2+} , and Mg^{2+} . The titration method was used for HCO_3^- analyses and the remaining major anions (Cl^- , SO_4^{2-} , and NO_3^-) were analyzed using an ultraviolet spectrophotometer.

The accuracy of the analysis was tested through the computation of electro neutrality using Equation (1), and the result show that the computed values range from 0.8% to 2.3%, which is in the acceptable range.

$$\text{ElectroNeutrality(E.N)}(\%) = \left[\frac{(\text{Sumcations} - \text{Sumanions})}{(\text{Sumcations} + \text{Sumanions})} \right] 100 \quad (1)$$

where the cations and anions are expressed as meq/L. The sums were taken over the cations Na^+ , K^+ , Mg^{2+} , and Ca^{2+} , and anions Cl^- , HCO_3^- , SO_4^{2-} , and NO_3^- .

The suitability of the analyzed water for irrigation was evaluated based on the sodium adsorption ratio (SAR), percentage sodium, magnesium hazard (MH), and electrical conductivities values of the waters at 25 °C (EC_{25}).

$$\text{SAR} = \frac{\text{Na}^+}{\sqrt{\frac{\text{Ca}^{2+} + \text{Mg}^{2+}}{2}}} \quad (2)$$

$$\% \text{Na} = \frac{\text{Na}^+}{\text{Ca}^{2+} + \text{Mg}^{2+} + \text{Na}^+ + \text{K}^+} \times 100 \quad (3)$$

$$\text{MH} = \frac{\text{Mg}^{2+}}{\text{Ca}^{2+} + \text{Mg}^{2+}} \times 100 \quad (4)$$

where all the ionic concentrations are expressed in milliequivalents per liter (meq/L) of the respective ion.

The field measured electrical conductivities values were measured at a temperature different from 25 °C and because of this a conversion of the field measured electrical conductivities values to EC_{25} at 25 °C were done using the appropriate conversion factors.

In this study, FAO guideline by Ayers and Westcot [37] was used to assess the salinity, sodicity, and toxicity impact of the analyzed water samples.

To determine the mechanism of salinization and water–rock interaction bivariate graphs of the parameters Ca^{2+} , Mg^{2+} , HCO_3^- , and SO_4^{2-} and computations of Na^+/Cl^- and $\text{Na}^+/\text{Na}^+ + \text{Cl}^-$ ratios and chloro-alkaline indices were used.

Chloro-alkaline indices (CAIs) were computed using the using the following formulas [38,39]:

$$\text{CAI 1} = \frac{[\text{Cl} - (\text{Na} + \text{K})]}{\text{Cl}} \quad (5)$$

$$\text{CAI 2} = \frac{[\text{Cl} - (\text{Na} + \text{K})]}{(\text{SO}_4 + \text{HCO}_3 + \text{CO}_3 + \text{NO}_3)} \quad (6)$$

3. Results

3.1. Water Balance

The computed water balance for the different parts of the catchment by Nata et al. [27] is summarized and given in the Table 1 below. The average annual rainfall in Gumselasa catchment is 485.89 mm: 84% of this amount is contributed by the three months of the rainy season (July, August, and September).

Table 1. Summary of water balance based on soil type of the area.

Location	Area (km ²)	AET (×10 ⁶) m ³	P (×10 ⁶) m ³	Q _i (×10 ⁶) m ³	Q _o (×10 ⁶) m ³	I (×10 ⁶) m ³
EWSSCL	17.16	5.468	8.34		1.167	1.705
EWSC	4.98	1.55	2.42		0.44	0.43
RES	0.4	0.505	0.194	1.607	0.553	0.743
WCA-1	0.55	0.19	0.267		0.048	0.029
WCA-2	3.99	1.42	1.94		0.349	0.171
CA	1	0.32	0.486	0.95	0.13	0.986

Where, EWSSCL is effective watershed with sandy loam soil; EWSC is effective watershed with clay soil; RES is reservoir; WCA-1 is water contributing area 1 with clay soil; WCA-2 is water contributing area 2 with clay soil; CA is command area; AET is actual evapotranspiration (AET for the reservoir is evaporation from the reservoir); P is mean annual rainfall; Q_i is input discharge (inflow); Q_o is runoff (outflow); and, I is infiltration, the amount of water that percolates into the upper level of groundwater as a groundwater accretion.

The construction of the dam has increased the availability of water in the catchment by harvesting the water especially that received during the rainy months of July to September, which accounts about 84% of the mean annual rainfall of the catchment. This might have led to an increment of the groundwater potential of the area by increasing the recharge.

The water that percolates as a recharge into the ground in the effective watershed area makes its way toward the command area beneath the dam as a groundwater flow together with the water of the dam that percolate deep as a recharge into the ground at the reservoir site. The water that percolates deep as a recharge at the water contributing area-1 and at the water contributing area-2 will also make their respective way toward the outlet of the catchment, which is the command area (Figure 1) following the direction of the water flow. All these are additional water to the command area on top of its own direct recharge amount.

The water balance computation analyses revealed that the overall infiltration in the Gumselasa catchment was 4.064 million cubic meters and 75.7% of this amount was flowing toward the command area following the direction of the water flow from a different direction of the catchment as a groundwater accretion. This augments the availability of groundwater in the command area and raised the level of groundwater toward the surface. As it was observed from the pits drilled in the command area, the groundwater level ranges from 0.2 to 2 m below the earth surface (Figure 7). With the exception of the deep borehole that is used for the domestic purpose, at present the groundwater in the command area is not used for any other purposes. Application of water for irrigation from the reservoir should take into account this readily available water in the irrigated area.

3.2. Hydrochemical Analyses

The water samples were analyzed for major cations and anions and the result is given in Table 2 and Figure 8. In the effective watershed of the catchment, 80% of the water was fresh and alkaline whereas the remaining 20%, which were mainly groundwater, were brackish and alkaline. The dominant anion was SO₄²⁻ and the dominant cation was Ca²⁺. In the analyzed groundwater, based on the mean values of the constituents, the cations were in the order of abundance as Ca²⁺ > Na⁺ > Mg²⁺ > K⁺. Anions content indicates that 60% of the analyzed groundwater samples followed the trend of SO₄²⁻ > HCO₃⁻ > Cl⁻ > NO₃⁻ and in the remaining 40% HCO₃⁻ > SO₄²⁻ > Cl⁻ > NO₃⁻. However, in the river water sample, the cations were in the order of abundance as Mg²⁺ > Na⁺ > Ca²⁺ > K⁺ and the anions were in the order of abundance as HCO₃⁻ > SO₄²⁻ > Cl⁻ > NO₃⁻.

Table 2. The chemical analyses of the groundwater, river water, and dam water in Gumselasa catchment.

Sample ID	Major Cations (mg/L)				Major Anions (mg/L)				Chemical Parameters		Water Type
	Na ⁺	K ⁺	Ca ²⁺	Mg ²⁺	Cl ⁻	SO ₄ ²⁻	NO ₃ ⁻	HCO ₃ ⁻	pH	TDS	
EWS 1	44	1.31	123	25	13.95	208.1	17.15	222	8.22	504	Ca-Mg-Na-SO ₄ -HCO ₃
EWS 2	51	1.07	104	20	18.95	247.4	14.9	375.9	8.35	472	Ca-Na-HCO ₃ -SO ₄
EWS 3	41	1.93	169	20	144.6	222.4	18.26	266.1	7.94	596	Ca-SO ₄ -HCO ₃ -Cl
EWS 4	48	1.16	127	19	13.07	235.1	16.33	344.3	8	588	Ca-HCO ₃ -SO ₄
EWS 5	70	1.09	83	23	44.25	256.1	19.15	297.2	8.42	668	Ca-Na-SO ₄ -HCO ₃
EWS 6	135	1.67	296	51	89.03	348.1	42.08	259.9	7.97	2189	Ca-Na-Mg-SO ₄ -HCO ₃
EWS 7	120	1.23	117	30	78.98	303.9	27.94	307.5	8.07	1193	Ca-Na-SO ₄ -HCO ₃
EWS 8	85	1.44	99	29	40.17	279.2	21.07	303.5	8.4	689	Ca-Na-Mg-SO ₄ -HCO ₃
EWS 9	55	1.06	157	16	43.01	95.3	17.99	133.3	7.82	358	Ca-Na-HCO ₃ -SO ₄
CA 1	161	1.91	487	169	83.77	186.6	46.74	372.1	7.81	5605	Ca-Mg-Na-HCO ₃
CA 2	107	1.42	202	35	63.08	353.3	45.09	495.7	7.95	1061	Ca-Na-HCO ₃ -SO ₄
CA 3	87	1.67	251	39	59.53	271.7	40.36	380.8	7.96	1059	Ca-Na-HCO ₃ -SO ₄
CA 4	124	1.78	213	54	39.79	341.1	18.57	203.1	8.33	1508	Ca-Na-Mg-SO ₄ -HCO ₃
CA 5	53	1.07	81	27	22.47	315	16.03	295	8.12	635	Ca-Na-Mg-SO ₄ -HCO ₃
CA 6	106	1.13	261	52	33.04	299.2	17.26	372.5	8.18	1266	Ca-Na-Mg-SO ₄ -HCO ₃
CA 7	119	1.99	371	79	47.18	377	20.55	216.7	8.13	1612	Ca-Mg-Na-SO ₄
CA 8	144	2.16	267	145	47.93	418.4	20.19	287.7	8.52	3016	Ca-Mg-Na-SO ₄ -HCO ₃
RW	70	1.13	11	38	40.93	119.4	15.17	246.1	8.42	662	Mg-Na-HCO ₃ -SO ₄
DW	18	1.04	15	9	39.89	87.82	13.89	211	8.2	248	HCO ₃ -SO ₄ -Cl

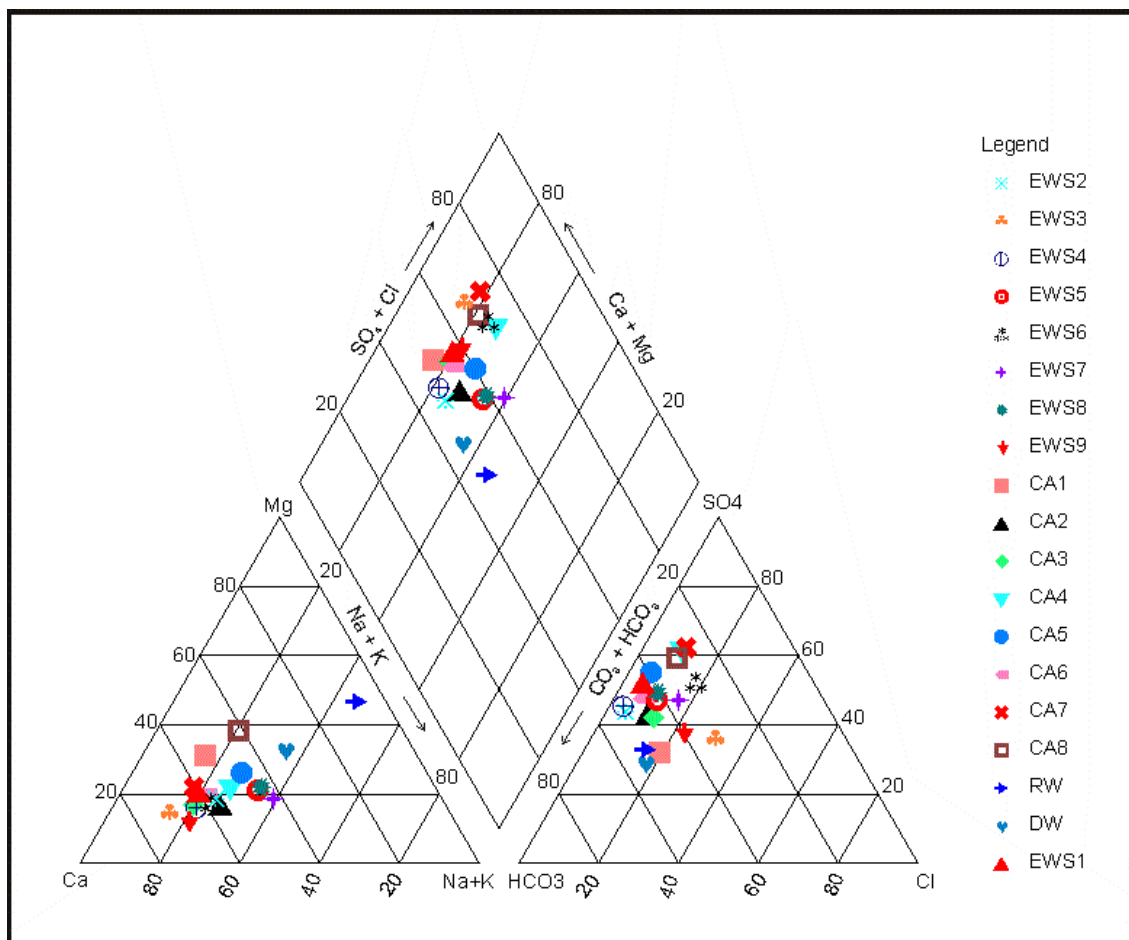


Figure 8. Piper diagram of the analyzed water samples.

Seven water types were recognized in the effective watershed area: Ca-Mg-Na-SO₄-HCO₃ (10%), Ca-SO₄-HCO₃-Cl (10%), Ca-HCO₃-SO₄ (10%), Mg-Na-HCO₃-SO₄ (10%), Ca-Na-SO₄-HCO₃ (20%), Ca-Na-HCO₃-SO₄ (20%), and Ca-Na-Mg-SO₄-HCO₃ (20%).

The dam water is fresh and alkaline having a dominant anion of HCO₃⁻ and SO₄²⁻ and dominant cations of Na⁺ and Ca²⁺. Generally, based on the mean values of the chemical parameters, the anions were in the order of abundance as HCO₃⁻ > SO₄²⁻ > Cl⁻ > NO₃⁻ and the cations were in the order of abundance as Na⁺ > Ca²⁺ > Mg²⁺ > K⁺. The water type is HCO₃-SO₄-Cl.

In the command area, with the exception of one sample that was fresh and alkaline, the groundwater was brackish and alkaline. The dominant anion was SO₄²⁻ and the dominant cation was Ca²⁺. In the analyzed groundwater samples 62.5% of the cations were in the order of abundance as Ca²⁺ > Na⁺ > Mg²⁺ > K⁺ and the anions were in the order of the abundance as SO₄²⁻ > HCO₃⁻ > Cl⁻ > NO₃⁻. In the remaining 37.5% the cations were in the order of the abundance as Ca²⁺ > Mg²⁺ > Na⁺ > K⁺ and the anions were in the order of abundance as HCO₃⁻ > SO₄²⁻ > Cl⁻ > NO₃⁻.

The water types recognized in the command area are Ca-Mg-Na-HCO₃ (12.5%), Ca-Mg-Na-SO₄ (12.5%), Ca-Mg-Na-SO₄-HCO₃ (12.5%), Ca-Na-HCO₃-SO₄ (25%), and Ca-Na-Mg-SO₄-HCO₃ (37.5%).

3.3. Irrigation Water Quality

Irrigation water assessment indices (SAR, %Na and MH) were computed for all the analyzed water samples and the results are given in Table 3.

Table 3. Computed irrigation parameters for groundwater, river water, and dam water samples in Gumselasa catchment.

Sample Id	EC ₂₅ at 25 °C (dS/m)	SAR	%Na	MH (%)
EWS 1	0.7	0.943	18.84	25.12
EWS 2	0.662	1.201	24.42	24.12
EWS 3	0.836	0.793	14.95	16.37
EWS 4	0.824	1.052	20.86	19.75
EWS 5	0.937	1.751	33.41	31.34
EWS 6	3.07	1.906	23.59	22.14
EWS 7	7.684	2.561	38.5	29.72
EWS 8	0.967	1.933	33.42	32.61
EWS 9	0.923	1.117	20.66	14.43
CA 1	7.68	1.601	15.47	36.4
CA 2	1.489	1.826	26.35	22.22
CA 3	1.485	1.348	19.33	20.39
CA 4	2.114	1.964	26.28	29.46
CA 5	0.89	1.306	26.86	35.46
CA 6	1.776	1.567	21.01	24.74
CA 7	2.26	1.465	17.13	25.99
CA 8	4.23	1.762	19.83	47.25
RW	0.929	2.242	45.04	85.05
DW	0.348	0.904	33.91	49.66

3.3.1. Salinity of Water

The salt concentration was determined by measuring the electrical conductivity (EC₂₅) of the water samples (Table 3). Accordingly, out of the analyzed nineteen water samples, four water samples have an EC₂₅ value greater than 3 dS/m, 13 water samples with EC₂₅ value ranging from 3 to 0.7 dS/m and the remaining two water samples had an EC₂₅ value less than 0.7 dS/m.

Based on the measured EC₂₅ values, the dam water and a groundwater sample from the effective watershed area (EWS2) were not hazardous and need no restriction on use. They can be used for almost all crops and for almost all kinds of soils [40]. This quality nature of the Gumselasa dam water is also shared by the other dams that are found in the

nearby areas such as dam Maylaey (0556650 mE/1461427 mN having an EC of 393 $\mu\text{S}/\text{cm}$) and dam May Gassa (0554732 mE/1460249 mN having 257.3 $\mu\text{S}/\text{cm}$) [29].

Thirteen samples, six from the command area and seven from the effective watershed area (including the river water), were unsafe and need a slight to moderate degree of restriction in the use of them. A continuous use of these waters for irrigation can cause a gradual increase of the salinity problem. The remaining four samples, two from the effective watershed area (EWS6 and EWS7) and two from the command area (CA1 and CA8), were severely saline waters. Continuous irrigation with such water might cause increasing to immediate salinity problems. They need restrictions in the use of them.

Based on this salinity nature analyses of the water three types of waters were recognized in the effective watershed area (including the river water) of the catchment: non-saline (10%), saline (70%), and severely saline (20%). The water in the dam was non-saline whereas in the command area two types of groundwater were identified: saline (75%) and severely saline (25%). Generally, the analyses of the results revealed that the severity of the salinity of water was high in the command area, implying an increasing degree of salinity toward the command area following the direction of the water flow.

3.3.2. Sodicity Hazard

The sodicity hazard was determined considering both the electrical conductivity (EC_{25}) and sodium adsorption ratio (SAR) together. The computed SAR values for all samples were less than 3 (Table 3). On the basis of measured EC_{25} values, two groups of water were identified in the study area: water that had an EC_{25} greater than 0.7 dS/m and water that had an EC_{25} values ranging from 0.7 to 0.2 dS/m. Sixteen samples, all the groundwater samples from the command area and eight from the effective watershed area (seven groundwater and a river water samples), were in the first group and need no restriction for use whereas three samples, two from the effective watershed (EWS1 and EWS2), and the dam water, were in the second group, which needs a slight to moderate degree of restriction in use of them.

The result of the analyses revealed that the groundwater in the effective watershed area was characterized by non-sodic and sodic nature. The river water was non-sodic whereas the dam water was sodic. The groundwater in the command area was characterized by non-sodic nature.

Sodium hazard was also evaluated using the percentage of sodium (Equation (3)). Based on the percentage of sodium the water was classified as excellent (<20%), good (20–40%), permissible (40–60%), doubtful (60–80%), and unsuitable (>80%) [41]. Accordingly, the groundwater of the effective watershed area had excellent to good irrigation water quality whereas the river water had permissible irrigation water quality. The dam water had good irrigation water quality and the groundwater in the command area had an excellent to good irrigation water quality (Table 3). This analyses shows that there was no water that had doubtful and unsuitable quality for irrigation.

Both the sodium adsorption ratio and percentage of sodium methods revealed that sodicity or sodium hazard did not increase from the effective watershed area to the command area following the direction of the water flow. Excess of sodium in irrigation water can affect the flow rate, permeability, infiltration, and soil structure promoting soil dispersion [42].

3.3.3. Magnesium Hazard (MH)

The degree of impact of magnesium in irrigation water to the soil structure is measured by the magnesium hazard (MH) [43]. Soil alkalinity can be caused by high concentration of Mg^{2+} in groundwater; additionally, between magnesium and clay particles a huge volume of water can be absorbed that decreases the infiltration capacity of the soil, which has an adverse impacts on crops [44–46]. According Abdulhussein [47] groundwater that has MH less than 50% is safe for irrigation whereas a MH greater than 50% is harmful and unsafe for irrigation.

The MH in the groundwater of the study area ranged from 14.43% to 47.25%, with a mean of 26.91% (Table 3). The MH of the dam water was also less than 50% whereas the river water in the effective watershed area of the catchment had a MH of greater than 50% and was unsafe for irrigation. The groundwater and the dam water are safe for irrigation.

3.3.4. Toxicity Hazard

The toxicity problem was assessed by measuring the concentrations of sodium. Accordingly, twelve water samples (four from the effective watershed area and seven from the command area and river water) had concentrations of sodium ranging from 3 to 9 meq/L, signifying that the water was slightly to moderately toxic whereas the remaining seven water samples (five from the effective watershed area and one from command area and dam water) had a concentrations sodium less than 3 meq/L indicating that the water was not toxic.

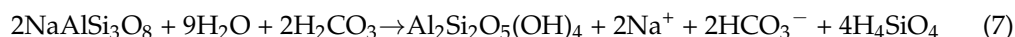
The groundwater in the effective watershed area was characterized by free to toxic nature. The river water had toxic nature whereas the dam water was free of any toxicity problem. The groundwater in the command area was dominantly toxic. In general, the trend of toxicity hazard increased from the effective watershed to the command area following the direction of the water flow.

4. Discussions

Sources of Salinity

Computed ionic ratios and chloro-alkaline indices values for the groundwater samples are given in the table below.

According to Golchin and AzhdaryMoghaddam [48], the ratio of Na^+/Cl^- can be used to determine the mechanism of salinization. The Na^+/Cl^- ratio of groundwater sampled ranging from 0.436 to 5.649 with a mean of 3.372 (Table 4). Of the total sample 89.5% show that the Na^+/Cl^- ratio was above 1 implying that dissolution of halite might not be the main source of Na^+ ions in the groundwater of the area. According to Mayback [49] and Elango and Kannan [50] this high concentrations of Na^+ than Cl^- normally interpreted as Na^+ released from silicate weathering as given below (Equation (7)).



The $\text{Na}^+/\text{Na}^+ + \text{Cl}^-$ ratio of the groundwater sampled was ranging from 0.304 to 0.85 with a mean of 0.739. With the exception of a groundwater sample from the effective watershed area (EWS3), all the remaining samples had a $\text{Na}^+/\text{Na}^+ + \text{Cl}^-$ ratio above 0.6, revealing that the source of Na^+ ions in the groundwater was primarily from incongruent dissolution of silicate minerals and cation exchange [51]. Figure 9 below shows a good correlation of Na^+ ions ($R^2 = 0.74$) with the total cations, suggesting possible sources from silicate minerals.

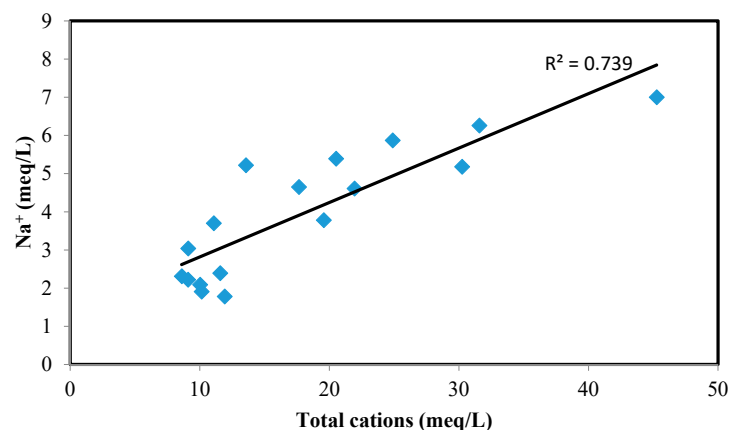


Figure 9. Na^+ versus total cations (meq/L) in the groundwater of the catchment.

Table 4. Computed values of Na^+/Cl^- and $\text{Na}^+/\text{Na}^+ + \text{Cl}^-$ ratios and chloro-alkaline indices for the analyzed groundwater in the Gumselasa catchment.

Sample Code	Na^+/Cl^-	$\text{Na}^+/\text{Na}^+ + \text{Cl}^-$	CAI1	CAI2
EWS1	4.897	0.830	−3.974	−0.189
EWS2	4.189	0.807	−3.245	−0.150
EWS3	0.436	0.304	0.551	0.244
EWS4	5.649	0.850	−4.730	−0.163
EWS5	2.432	0.709	−1.456	−0.174
EWS6	2.339	0.700	−1.355	−0.282
EWS7	2.341	0.701	−1.354	−0.257
EWS8	3.274	0.766	−2.310	−0.236
EWS9	1.975	0.664	−1	−0.275
CA1	2.966	0.748	−1.987	−0.443
CA2	2.612	0.723	−1.635	−0.181
CA3	2.25	0.692	−1.274	−0.172
CA4	4.813	0.828	−3.857	−0.404
CA5	3.667	0.786	−2.714	−0.147
CA6	4.957	0.832	−3.989	−0.296
CA7	3.895	0.796	−2.932	−0.334
CA8	4.637	0.823	−3.681	−0.363
Minimum	0.436	0.304	−4.730	−0.443
Maximum	5.649	0.850	0.551	0.244
Average	3.372	0.739	−2.408	−0.225

The low chloride ions concentration in the groundwater of the catchment was due to lack of natural sources in the area.

To gain more insight about the ion exchange processes, computation of chloro-alkaline indices (CAIs) for the sampled groundwater were carried out (Table 4). According to Schoeller [39] chloro-alkaline indices (CAI) is used to recognize the ion exchange between groundwater and its aquifer during residence time within the aquifer. As shown in the Table 4, 94% of the samples had negative CAI1 values and 6% had positive values. CAI1 ranged from −4.73 to 0.551 with a mean of −2.408. CAI2 ranged from −0.443 to 0.244 with a mean of −0.225. Of the total samples 94% had a negative CAI2 values and 6% had a positive CAI 2 values. This great percentage of negative chloro-alkali indices value revealed the existence of an exchange Mg^{2+} and Ca^{2+} of the groundwater with Na^+ and K^+ ions from rocks. In the 6% of the total samples, however, the reverse ion exchange process was the significant one.

The plot of $(\text{Ca}^{2+} + \text{Mg}^{2+} - \text{SO}_4^{2-} - \text{HCO}_3^-)$ versus $(\text{Na}^+ - \text{Cl}^-)$ was used to determine whether the cation exchange was a major mechanism of salinization or not [52]. As shown in the Figure 10, the relation between these two parameters were not linear ($r^2 = 0.32$), signifying that cation exchange was not a significant mechanism of salinization in the catchment.

A plot of $\text{Ca}^{2+} + \text{Mg}^{2+}$ versus $\text{SO}_4^{2-} + \text{HCO}_3^-$ (Figure 11) was used to determine the role of congruent dissolution minerals (calcite, dolomite, and gypsum) and incongruent dissolution of silicate minerals as a mechanism of salinization in the studied area. According to Datta and Tyagi [53] a scatter diagram of $(\text{Ca}^{2+} + \text{Mg}^{2+})$ versus $(\text{SO}_4^{2-} + \text{HCO}_3^-)$ can be used for this purpose. As shown in the Figure 11, 52.9% of the total samples were laying above the equiline, revealing that congruent dissolution of carbonate minerals and gypsum were the prevailing composition-controlling processes whereas in those samples below the equiline, which constituted 41.2% of the total samples, incongruent dissolution of silicate minerals was the dominant process. In the sample that fell along the equiline (EWS1; 5.9% of the total sample) was due to both dissolution of carbonate minerals (including gypsum) and silicate weathering. This indicates that dissolution of carbonate minerals and

gypsum (Equations (8)–(10)) was the main source for Ca, Mg, and SO₄ ions [50,51,54] in groundwater of the catchment.

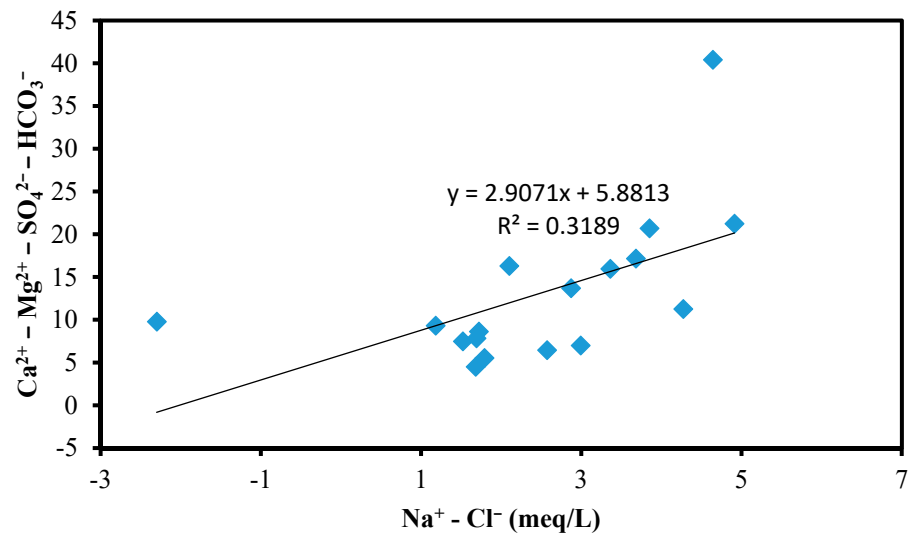
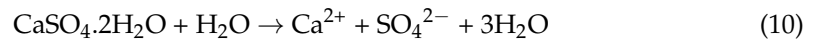
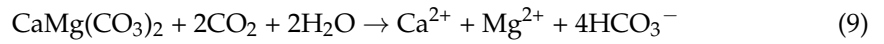
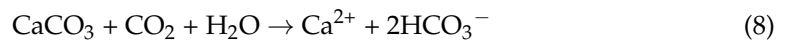


Figure 10. $\text{Ca}^{2+} + \text{Mg}^{2+} - \text{SO}_4^{2-} - \text{HCO}_3^-$ versus $\text{Na}^+ - \text{Cl}^-$ in the groundwater of the catchment.

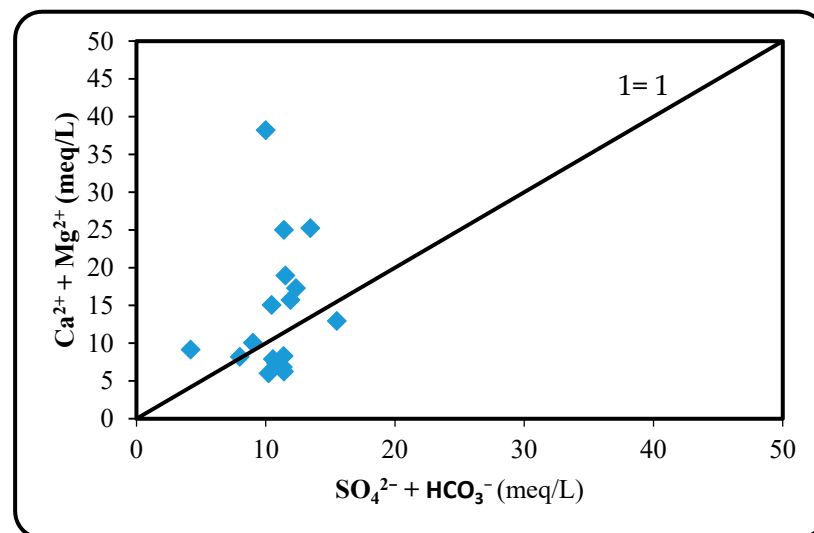


Figure 11. $\text{Ca}^{2+} + \text{Mg}^{2+}$ versus $\text{SO}_4^{2-} - \text{HCO}_3^-$ in the groundwater of the catchment.

The plot of Ca^{2+} versus SO_4^{2-} (Figure 12a) and Ca^{2+} versus HCO_3^- (Figure 12b) are portraying the existence of higher concentration of Ca^{2+} over SO_4^{2-} and HCO_3^- , respectively. This high concentration of Ca^{2+} revealed the presence of additional source for Ca^{2+} besides to the dissolution of carbonate minerals. This additional source is the incongruent dissolution of silicate weathering [55], which is also a source of bicarbonate ions to the groundwater of the catchment. In this reaction, plagioclase feldspar (anorthite) minerals

react with carbonic acid in the presence of water and releases calcium and bicarbonate ions into the groundwater [56] (Equation (11)).

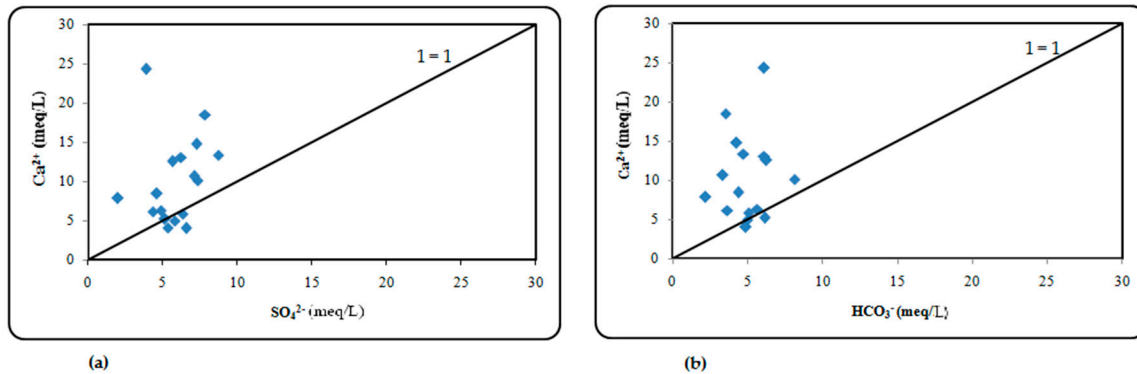
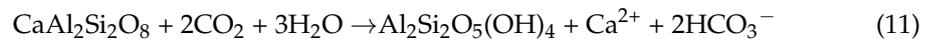


Figure 12. (a) Ca^{2+} versus SO_4^{2-} and (b) Ca^{2+} versus HCO_3^- in the groundwater of the catchment.

In conclusion all the above computations of ratios and chloro-alkaline indices and bivariate plots depict that silicate weathering, dissolution of carbonate minerals, and gypsum and ion exchange are the major geochemical processes that control the groundwater chemistry in the studied area. Among these, however, the significant composition-controlling processes or salinization mechanisms are dissolution of carbonate minerals and gypsum and silicate weathering.

5. Conclusions

Limestone–shale–marl intercalation with dolerite intrusion and Quaternary sediments are the geological formations that constituted the catchment. The rate of flow of the groundwater and its quality is profoundly affected by these formations as the groundwater flow from different parts and directions of the catchment toward the command area. Due to the impervious nature of the intercalated shale and poorly weathered and fractured nature of the dolerite, the rate of flow of groundwater through these formations is very sluggish, resulting in a high circulation period and longer residence time. This creates an opportunity for different water–rock interaction processes to take place invariably and modify the quality of the groundwater. Calcite and gypsum from the intercalated limestone is easily affected by a congruent dissolution process while the different silicate minerals in the dolerite and dissolved and recrystallized calcium carbonate (caliche) on the surface of dolerite are affected invariably by both congruent dissolution carbonate (calcite, dolomite, and gypsum) and incongruent dissolution of silicate minerals.

The surface waters and groundwater in the Gumselasa catchment were evaluated for their chemical composition and suitability for irrigation. The abundance of the major ions in the majority of the groundwater of the effective watershed area was as follows: $\text{Ca}^{2+} > \text{Na}^+ > \text{Mg}^{2+} > \text{K}^+$ and $\text{SO}_4^{2-} > \text{HCO}_3^- > \text{Cl}^- > \text{NO}_3^-$. In the river water the abundance of the major ions is $\text{Mg}^{2+} > \text{Na}^+ > \text{Ca}^{2+} > \text{K}^+$ and $\text{HCO}_3^- > \text{SO}_4^{2-} > \text{Cl}^- > \text{NO}_3^-$. The abundance of the major ions in the dam water was $\text{Na}^+ > \text{Ca}^{2+} > \text{Mg}^{2+} > \text{K}^+$ and $\text{HCO}_3^- > \text{SO}_4^{2-} > \text{Cl}^- > \text{NO}_3^-$. In the command area the abundance of the major ions in the majority of the groundwater was as follows: $\text{Ca}^{2+} > \text{Na}^+ > \text{Mg}^{2+} > \text{K}^+$ and $\text{SO}_4^{2-} > \text{HCO}_3^- > \text{Cl}^- > \text{NO}_3^-$.

Hydrochemical analyses revealed that in the effective watershed area of the catchment, groundwater was dominantly fresh and alkaline and the main hydrochemical facies are Ca-Na- SO_4 - HCO_3 , Ca-Na- HCO_3 - SO_4 , and Ca-Na-Mg- SO_4 - HCO_3 . The river water was fresh and alkaline and the water is the Mg-Na- HCO_3 - SO_4 type. The dam water was fresh and alkaline and the water is HCO_3 - SO_4 -Cl type. In the command area the groundwater

was dominantly brackish and alkaline and the main hydrochemical facies were Ca-Na-HCO₃-SO₄ and Ca-Na-Mg-SO₄-HCO₃.

Irrigation water quality analyses revealed that salinity and toxicity show an increasing tendency from the effective watershed area towards the command area following the direction of the water flow. The results also showed that the analyzed waters for irrigation purpose had no sodicity hazard.

The increment of the availability of groundwater due to the existing dam enhanced dissolution of carbonate minerals (calcite, dolomite, and gypsum), silicate weathering, and cation exchange processes, which are the main causes of salinity in the irrigated land. Among these salinization mechanisms, the most influential are carbonate and silicate weathering processes. The rising of the saline groundwater combined with insufficient leaching contributed to secondary salinization development in the command area of the Gumselasa irrigation scheme.

Currently more than 10 ha land of the command area was abandoned because of salinization in the studied area. The following general recommendations were forwarded in order to minimize risk of salinization and salt accumulation in the soils of the command area:

- Surface and subsurface drainages must be installed to minimize groundwater rise that lead to salinization due to salts dropped in soil when the rise up groundwater evaporates and;
- Salt tolerant (salt loving) plants should be planted in areas where there is high salinity, like rice, barley, and other salt tolerant plants.

Author Contributions: M.G., N.T.T., and S.H. study design, methodology, performed the fieldwork, analyzed the data, and wrote the paper; B.F.A., K.L., and R.L. revised the manuscript. All authors have read and agreed to the published version of the manuscript.

Funding: This research was funded by European Union and African Union: Under the EAU4Food-Mekelle University.

Data Availability Statement: Data is contained within the article.

Acknowledgments: Financial support for this study was provided by European Union and African Union: Under the EAU4Food-Mekelle University. It is gratefully acknowledged.

Conflicts of Interest: The authors declare no conflict of interest.

References

1. Zaman, M.; Shahid, S.A.; Heng, L. *Guideline for Salinity Assessment, Mitigation and Adaptation Using Nuclear and Related Techniques*; Springer Nature AG: Cham, Switzerland, 2018; p. 162. ISBN 978-3-319-96189-7.
2. Evangelou, V.P. *Effect of Fertilizer Salts on Crop Production*; Soil Science News and Views: Lexington, KY, USA, 1983; p. 164. Available online: https://uknowledge.uky.edu/pss_views/164 (accessed on 25 December 2020).
3. Szabolcs, I. *Salt-Affected Soils*; CRC Press: Boca Raton, FL, USA, 1989; p. 274.
4. Pooja, S.; Rajesh, K. Soil salinity: A serious environmental issue and plant growth promoting bacteria as one of the tools for its alleviation. *Saudi J. Biol. Sci.* **2015**, *22*, 123–131.
5. Massoud, F.I. Salinity and alkalinity. In *A World Assessment of Soil Degradation: An International Program of Soil Conservation*; Report of an expert consultation on soil degradation; FAO: Rome, Italy, 1974; pp. 16–17.
6. Ponnampuruma, F.N. Role of cultivar tolerance in increasing rice production on saline-lands. In *Salinity Tolerance in Plants: Strategies for Crop Improvement*; Staple, R.C., Toenniessen, G.H., Eds.; Wiley: New York, NY, USA, 1984; pp. 255–271.
7. Mateo-Sagasta, J.; Burke, J. Agriculture and water quality interactions: A global overview. In *SOLAW Background Thematic Report—TR08*; FAO: Rome, Italy, 2011; p. 46.
8. Stanners, D. *Europe's Environment: The Dobbris Assessment*; Office for Official Publication of the European Communities: Luxembourg, 1995.
9. Taddese, G. Land degradation: A Challenge to Ethiopia. *Environ. Manag.* **2001**, *27*, 815–824. [[CrossRef](#)]
10. Ruffeis, D.; Loiskandl, W.; Spendlingwimmer, R.; Schonerlee, M.; Awulachew, S.B.; Boelee, E.; Wallner, K. Environmental impact analysis of two large scale irrigation schemes in Ethiopia. In *Proceedings of the Impact of Irrigation on Poverty and Environment in Ethiopia: Draft Proceedings of the Symposium and Exhibition*, Addis Ababa, Ethiopia, 27–29 November 2007; Awulachew, S.B., Loulseged, M., Yilma, A.D., Eds.; International Water Management Institute (IWMI): Colombo, Sri Lanka, 2008; pp. 370–388.
11. Gebrehiwot, K.A. A review on waterlogging, salinization and drainage in Ethiopian irrigated agriculture. *Sustain. Water Resour. Manag.* **2018**, *4*, 55–62. [[CrossRef](#)]

12. Abebe, T.F.; Alamirew, T.; Abegaz, F. Appraisal and mapping of soil salinity problem in Amibara irrigation farms, Middle Awash basin. *IJISR* **2015**, *13*, 298–314.
13. Hagos, E.Y.; Schultz, B.; Depeweg, H. Reservoir operation in view of effective utilization of limited water in semi-arid areas, the case of Gumselasa earthen dam irrigation scheme in Tigray. *Ethiopia. Irrigat. Drain.* **2016**, *65*, 294–307. [[CrossRef](#)]
14. Darout, G. The Socio-Cultural Aspect of Irrigation Management: The Case of Two Community-Based Small-Scale Irrigation Schemes in the Upper TEKEZE Basin, Tigray Region, Ethiopia. Master's Thesis, Addis Ababa University, Addis Ababa, Ethiopia, 2004; p. 126.
15. Teshome, W. Irrigation practices, state intervention and farmer's life-worlds in drought-prone Tigray. In *Best Practices and Technologies for Small Scale Agricultural Water Management in Ethiopia, Proceedings of the MoARD/MoWR/USAID/IWMI Symposium and Exhibition, Addis Ababa, Ethiopia, 7–9 March 2006*; Awulachew, S.B., Menker, M., Abesha, D., Atnafe, T., Wondimkun, Y., Eds.; IWMI: Colombo, Sri Lanka, 2006; pp. 129–142.
16. Mintesinot, B. Assessment and Optimization of Traditional Irrigation of Vertisols in Northern Ethiopia: A Case Study at Gumselasa Micro-Dam Using Maize as an Indicator Crop. Ph.D. Thesis, Ghent University, Ghent, Belgium, 2002.
17. Yazew, E. *Development and Management of Irrigated Lands in Tigray, Ethiopia*; Balkema: Delft, The Netherlands, 2005; p. 265. ISBN 04-1538-485-0.
18. Degol, F.Y.; Ritsema, C.J.; Solomon, H.; Froebrich, J.; van Dam, J.C. Irrigation water management: Farmers' practices, perceptions and adaptations at Gumselasa irrigation scheme, North Ethiopia. *Agric. Water Manag.* **2017**, *191*, 16–28.
19. Haregeweyn, N.; Poesen, J.; Nyssen, J.; De Wit, J.; Haile, M.; Govers, G.; Deckers, S. Reservoirs in Tigray (Northern Ethiopia): Characteristics and sediment deposition problems. *Land Degrad. Develop.* **2006**, *17*, 211–230. [[CrossRef](#)]
20. Fassile, K.; Charles, Y. Soil fertility status and NuMaSS fertilizer recommendation of typichaplusterts in the northern highlands of Ethiopia. *World Appsci. J.* **2009**, *6*, 1473–1480.
21. Degol, F. *Irrigation Water Management: Effects of Irrigation Water Management Practices on the Prognosis of Soil Salinization: Case Study of Farms around Gumselasa Dam, Tigray, Ethiopia*; VDM Verlag Dr. Müller: Riga, Latvia, 2010; p. 96.
22. Yordanos, B. Collective Action in Irrigation System Management: A Case Study on the Management of Two Irrigation Schemes in Tigray, Ethiopia. Master's Thesis, Wageningen University, Wageningen, The Netherlands, 2012; p. 77.
23. Tedros, T. Contribution of Small Holders' Irrigation to Households Income and Food Security: A Case Study of Gum-Selasa and Shilena Irrigation Schemes, Hintalowejerat, South-Eastern Zone of Tigray, Ethiopia. Master's Thesis, Mekelle University, Mekelle, Ethiopia, 2014.
24. Oates, N.; Hisberg, A.; Rodríguez Ros, J.; Solomon, H.; Ludi, E.; Marlet, S.; Jamin, J.-Y. The implications of state intervention for self-governed irrigation schemes: Insights from Tigray, Ethiopia. *Irrig. Drain.* **2020**, *69*, 88–99. [[CrossRef](#)]
25. Gebremedhin, B.; Tesfamichael, G.; Kristine, M.; Kristine, W. Overview of micro-dam reservoirs (MDR) in Tigray (northern Ethiopia): Challenges and benefits. *J. Afr. Earth Sci.* **2016**, *123*, 210–222.
26. Amdom, G.; Henok, S.; Amanuel, Z.; Girmay, G.; Solomon, H.; Tesfay, G. The impact of climate change on irrigation water requirement of Maize and Onion: The case of Gumselasa small-scale irrigation scheme, Tigray, Ethiopia. *J. Drylands* **2018**, *8*, 729–740.
27. Nata, T.T.; Michiele, G.; Solomon, H.; Berhanu, F.A. Water balance model: Implications for groundwater recharge estimation in data scarce arid catchment, northern Ethiopia. *Asian Rev. Environ. Earth Sci.* **2018**, *5*, 34–46.
28. Gebremedhin, G.; Gebremicael, T.G.; Mulubrehan, K.; Esayas, M.; Teferi, G.; Abbadi, G. Salinization pattern and its spatial distribution in the irrigated agriculture of northern Ethiopia: An integrated approach of quantitative and spatial analyses. *Agric. Water Manag.* **2018**, *206*, 147–157. [[CrossRef](#)]
29. Michiele, G. Assessment of Sources of Salinity in Gumselasa Irrigation Scheme, Southern Tigray, Ethiopia. Master's Thesis, Mekelle University, Mekelle, Ethiopia, 2014; p. 78.
30. Nata, T. Lithological and structural controls on the development of aquifer in basement rock dominated Tsalit-Ira river basin, Tigray, Northern Ethiopia. *Momona Ethiop. J. Sci.* **2017**, *9*, 106–126.
31. Alemu, T.; Abdelsalam, M.G.; Dawit, E.L.; Atnafu, B.; Mickus, K.L. The Paleozoic e Mesozoic Mekele Sedimentary Basin in Ethiopia: An example of an exhumed IntraCONTinental Sag (ICONS) basin. *J. Afr. Earth Sci.* **2018**, *143*, 40–58. [[CrossRef](#)]
32. Beyth, M. Paleozoic-Mesozoic Sedimentary Basins of Mekele Outlier. Northern Ethiopia. *Assoc. Am. Pet. Geol. Bull.* **1972**, *56*, 2426–2439.
33. Engels, G.G. *Mesozoic Stratigraphy of Northern Ethiopia*, Rept. No. ETG-18. Unpublished Report. 1966.
34. Enkurie, D.L. Adigrat Sandstone in Northern and Central Ethiopia: Stratigraphy, Facies, Depositional Environments and Palynology. Ph.D. Thesis, University of Berlin, Berlin, Germany, 2010; p. 162.
35. Worash Getaneh. Sulfides, Stable isotopes and other Diagenetic features of the Mesozoic Carbonate-Marl-Shale Succession in Northern Ethiopia. *SINET Ethiop. J. Sci.* **2016**, *39*, 34–49.
36. Nata, T.; Miruts, H.; Bheemalingeswara, K. Hydrogeological Investigation: A case study on the groundwater potential assessment in the Hantebet catchment, Tigray, northern Ethiopia. *J. Drylands* **2009**, *2*, 55–65.
37. Ayers, R.S.; Westcot, D.W. *Water Quality for Agriculture*; FAO Irrigation and Drainage Paper 29 Rev.1; FAO: Rome, Italy, 1989; p. 156.
38. Faisal, K.Z.; Saad, M.; Manoj, M.; Elkhedr, I. Evaluation of groundwater chemistry and its impact on drinking and irrigation water quality in the eastern part of the Central Arabian graben and trough system, Saudi Arabia. *J. Afr. Earth Sci.* **2016**, *120*, 208–219.

39. Schoeller, H. Qualitative evaluation of groundwater resources. In *Methods and Techniques of Groundwater Investigation and Development*; Water Resource Series No. 33; Schoeller, H., Ed.; UNESCO: Paris, France, 1967; pp. 44–52.
40. Nata, T.; Bheemalingwara, K. Prospects and constraints of household irrigation practices, Hayelom watershed, Tigray, northern Ethiopia. *Momona Ethiop. J.Sci.* **2010**, *2*, 87–109. [[CrossRef](#)]
41. Carmelita, S.N.; Thushyanthy, M.; Barathithasan, T.; Saravanan, S. Irrigation water quality based on hydro chemical analysis, Jaffna, Sri Lanka. *Am. Eurasian J. Agric. Environ. Sci.* **2010**, *7*, 100–102.
42. Selma, E.; Semia, C.; Jamila, T. Hydrochemical assessment of water quality for irrigation: A case study of the Medjerda River in Tunisia. *Appl. Water Sci.* **2017**, *7*, 469–480.
43. Tahmasebi, P.; Mahmudy-Gharaie, M.H.; Ghassemzadeh, F.; Karouyeh, A.K. Assessment of groundwater suitability for irrigation in a gold mine surrounding area, NE Iran. *Environ. Earth Sci.* **2018**, *77*, 766. [[CrossRef](#)]
44. Ravikumar, P.; Somashekar, R.K.; Angami, M. Hydrochemistry and evaluation of groundwater suitability for irrigation and drinking purposes in the Markandeya River basin, Belgaum District, Karnataka State, India. *Environ. Monit. Assess.* **2011**, *173*, 459–487. [[CrossRef](#)] [[PubMed](#)]
45. Hussain, Y.; Ullah, S.F.; Akhter, G.; Aslam, A.Q. Groundwater quality evaluation by electrical resistivity method for optimized tube well site selection in an ago-stressed Thal Doab Aquifer in Pakistan. *Model. Earth Syst. Environ.* **2017**, *3*, 15. [[CrossRef](#)]
46. Khalid, S. An assessment of groundwater quality for irrigation and drinking purposes around brick kilns in three districts of Balochistan province, Pakistan, through water quality index and multivariate statistical approaches. *J. Geochem. Explor.* **2019**, *197*, 14–26.
47. Abdulhussein, F.M. Hydrochemical assessment of groundwater of Dibdibba aquifer in Al-Zubair area, Basra, south of Iraq and its suitability for irrigation purposes. *Iraqi J. Sci.* **2018**, *59*, 135–143.
48. Golchin, I.; AzhdaryMoghaddam, M. Hydro-geochemical characteristics and groundwater quality assessment in Iranshahr plain aquifer, Iran. *Environ. Earth Sci.* **2016**, *75*, 14. [[CrossRef](#)]
49. Mayback, M. Global chemical weathering of surficial rocks estimated from river dissolved loads. *Am. J. Sci.* **1987**, *287*, 401–428. [[CrossRef](#)]
50. Elango, L.; Kannan, R. Rock–water interaction and its control on chemical composition of groundwater. In *Developments in Environmental Science*; Sarkar, D., Datta, R., Hannigan, R., Eds.; Elsevier: Amsterdam, The Netherlands, 2007; Volume 5, pp. 229–243.
51. Adomako, D.; Osaе, S.; Akiti, T.T.; Faye, S.; Maloszewski, P. Geochemical and isotopic studies of groundwater conditions in the Densu River Basin of Ghana. *Environ. Earth Sci.* **2011**, *62*, 1071–1084. [[CrossRef](#)]
52. Fisher, R.S.; Mullican, W.F. Hydrochemical evolution of sodium-sulfate and sodium-chloride groundwater beneath the northern Chihuahuan Desert, Trans-Pecos, Texas, USA. *Hydrogeol. J.* **1997**, *5*, 4–16. [[CrossRef](#)]
53. Datta, P.S.; Tyagi, S.K. Major ion chemistry of groundwater in Delhi area: Chemical weathering processes and groundwater flow regime. *J. GeolSoc. India* **1996**, *47*, 179–188.
54. Garrels, R.M. A survey of low temperature water mineral relations. In *Interpretation of Environmental Isotope and Hydrogeochemical Data in Groundwater Hydrology*; International Atomic Energy Agency: Vienna, Austria, 1976; pp. 65–84.
55. Zhang, B.; Song, X.; Zhang, Y.; Han, D.; Tang, C.; Yilei, Y.; Ma, Y. Hydrochemical characteristics and water quality assessment of surface water and groundwater in Songnen Plain, northeast China. *Water Res.* **2012**, *46*, 2737–2748. [[CrossRef](#)] [[PubMed](#)]
56. Elango, L.; Kannan, R.; Senthil Kumar, M. Major ion chemistry and identification of hydrogeochemical processes of groundwater in a part of Kancheepuram district, Tamil Nadu, India. *Environ. Geosci.* **2003**, *10*, 157–166.